

2D electron momentum distributions for transfer ionization in fast proton Helium collisions

M. S. Schöffler^{1,*}, O. Chuluunbaatar^{2,3}, S. Houamer⁴, A. Galstyan⁵,
J. N. Titze¹, L. Ph. H. Schmidt¹, T. Jahnke¹, H. Schmidt-Böcking¹,
R. Dörner¹, Yu. V. Popov⁶, A.A. Gusev², and C. Dal Cappello⁷

¹ *Institut für Kernphysik, University Frankfurt,
Max-von-Laue-Str. 1, 60438 Frankfurt, Germany*

² *Joint Institute for Nuclear Research,
Dubna, Moscow region 141980, Russia*

³ *School of Mathematics and Computer Science,
National University of Mongolia, UlaanBaatar, Mongolia*

⁴ *Département de physique, Faculté des Sciences,
Université Ferhat Abbas, Sétif, 19000, Algeria*

⁵ *Faculty of Physics, Lomonosov Moscow State University, Moscow 119991, Russia*

⁶ *Skobeltsyn Institute of Nuclear Physics,
Lomonosov Moscow State University, Moscow 119991, Russia and*

⁷ *Institut de Chimie, Physique et des Matériaux,
Université de Lorraine 1 Bd Arago 57078 METZ Cedex 3, France*

(Dated: May 21, 2013)

Abstract

The momentum distribution of the electron in the reaction $p+\text{He} \rightarrow \text{H} + \text{He}^{2+} + e$ is measured for projectile energies $E_p=300$ and 630 keV/u at very small scattering angles of hydrogen. We mainly present two dimensional distributions parallel (k_{\parallel}) and perpendicular (k_{\perp}) to the projectile beam. Theoretical calculations were carried out within the Plane Wave First Born Approximation (PWFBA), which includes both electron emission mechanisms, shake-off and sequential capture and ionization. It is shown that electron correlations in the target wave function play the most important role in the explanation of experimentally observed backward emission. Second order effects have to be involved to correctly describe the forward emission of the electron.

*Electronic address: schoeffler@atom.uni-frankfurt.de

I. INTRODUCTION

In the past decade a new wave of theoretical and experimental interest in electron capture processes, involving two active electrons, as double capture (DC), transfer ionization (TI) and transfer excitation (TE), has shed light on the versatile effects of electron correlation. New experimental techniques allow to measure more than only total or single differential cross section (SDCS). Fully differential cross sections (FDCS), which depend on the momentum distribution of the escaped electron in TI give a rather detailed view in the dynamical processes taking place. In particular, in this paper we consider the reaction $p+\text{He} \rightarrow \text{H}+\text{He}^{2+}+e^{-}$.

Since the early publications [3, 4] it became clear that two principal mechanisms contribute to the transfer ionization. This takes place via a capture of one electron with a correlated (shake-off, SO) or sequential process (binary encounter, BE), removal of the second electron. We use this terminology in accord with single photon ionization of an atom [1, 2] in spite of quite different transfer energies in both cases. Let us concentrate further on the single transfer ionization, because this process is a subject of this paper. Direct capture presumes the "usurpation" of one target electron by the fast projectile proton, like it was described in [3], and releasing of another electron due to the sudden rearrangement of the field in the residual ion (typical SO). If the fast proton is described by the plane wave in the lab frame, and its scattering angles are very small (fractions of mrad), then the OBK-mechanism [3] presents the principal transition matrix element alike to that for Electron Momentum Spectroscopy [5] (see also [6]). In turn, it was shown that latter one is very sensitive to angular and radial electron-electron correlations in the target [7].

The captured electron always moves forward parallel to the velocity vector of the proton projectile, i.e. its momentum component is positive. If the electron-electron correlation in the target is weak (say, only due to a mean field), the emitted electron will be shaken off isotropically. In the opposite case of strong angular correlations it moves predominantly in backward direction ($k_{\parallel} < 0$) and we expect to see a backward peak in the electron momentum distribution. A different process (analogue to radiative electron capture) also resulting in a backward emitted electron was suggested by Voitkiv and coworkers [8, 9]. These calculations lack of high differentiability, as they are neither in the scattering angle dependent nor in the scattering plane. Therefore we will show our data only in the longitudinal vs. transversal

representation.

The sequential mechanism of TI presumes at least two successive interactions of the fast projectile with both target electrons. For its realization no electron–electron correlations are needed. This mechanism in general is of the second order (and higher) in the projectile–target interaction. However, features of the capture processes allow to define transfer ionization already with a first order amplitude [10]. After interaction of the bound electron with the fast projectile proton it becomes also fast. It can interact again with another electron or the target nucleus on its way out (pure second order $Ne-$ and ee -Thomas, for example [4, 11]), but its movement keeps in general the forward character $k_{||} > 0$. So, the forward peak can be connected with the BE mechanism; capture and ionization are generally independent.

Of course, the above considerations are semiclassical, we shall see an interplay of quantum mechanisms and coherent sum of corresponding matrix elements, but we expect the general forward-backward features to be present also in a full quantum treatment.

We think, it is a time to defend the PWFBA, because first Born theories are often believed to be inadequate for electron capture. We would like to stress that it is not so. First, any FBA theory works well until the higher Born terms become bigger in the region of final state phase space considered. So for example at very small scattering angles of a fast projectile ion (proton), the OBK term is a leading one but it falls down rapidly with increasing scattering angle, and the higher order terms begin to contribute. But they do not contribute much at very small angles (see calculations in [12]). Second, the OBK matrix element, as it was considered 80 years ago, now can include much better correlated trial wave functions. This plays a crucial role for transfer excitation and transfer ionization reactions (less for charge transfer). At very small projectile scattering angles, the corresponding SDCS curves for highly and loosely correlated target ground functions start to differ substantially. Third, we have now two main approaches for capture reaction: time-dependent semiclassical and pure quantum mechanical. Within the time-dependent approach the heavy fast projectile particle is considered a source of a classical outer field. The interaction of both, projectile and target ion, can easily be taken into account as a phase-factor to the final (initial) wave function [13]. In the pure quantum approach (see, for example, [12]) the interaction of heavy particles gives a contribution to the FBA, and this term distorts noticeably the OBK term both at very small (here the distortion is "positive", it diminishes the peak value) and at larger scattering angles (here this distortion is "negative", it increases the plateau). It was

shown that SBA terms can compensate this negative effect and considerably improve the agreement between theory and experiment [12]. Physically it is clear that if the transferred momentum and energy are relatively small (we are in a laboratory frame, and this takes place at very small scattering angles), then the velocity of atomic nucleus is practically zero, and it is actually immovable during the scattering process. The nucleus simply changes the initially directed path of the projectile due to elastic scattering ("secondary" OBK). This is the main physical role of this term at scattering angles close to zero. But its FBA realization distorts this picture at larger angles, and the SBA provides with necessary corrections.

In this paper we present experimental results and calculate fully differential cross sections (FDCS) within the plane wave first Born approximation (PWFBA) on proton-helium interaction at impact energies of 300 and 630 keV. Both discussed above mechanisms, SO and BE, contribute in this case.

Atomic units $\hbar = e = m_e = 1$ are used throughout unless otherwise specified.

II. EXPERIMENT

To achieve the goals of this experiment all emitted particles have to be measured in coincidence. Therefore we applied momentum spectroscopy techniques, as reactions microscopes or COLTRIMS (COLd Target Recoil Ion Momentum Spectroscopy) [15–17]. The experiments were performed at the Institut für Kernphysik at the University of Frankfurt using the Van de Graaff accelerator. Using 3 sets of movable slits, the proton beam was collimated to a divergence less than 0.15 mrad, an size of about $0.5 \times 0.5 \text{ mm}^2$ at the overlap region with the gas jet. 15 cm upstream of the target, a set of parallel electrostatic deflector plates cleaned the primary beam from charge state impurities, deflecting the primary beam slightly upwards. The H^+ beam was crossed perpendicular with the helium gas jet. 15 cm downstream of the target a second set of horizontal electrostatic deflector plates separate the final charge state, thus only the neutral projectiles H hit a position and time sensitive multichannel plate (MCP) detector, placed 3 m downstream the interaction point, yielding the projectile deflection angle and the time zero of the collision. The main part of the beam ($\approx 1 \text{ nA}$), which is still charged was dumped in a Faraday cup.

The gas jet providing the target beam was generated by helium gas expanding through a $30 \text{ }\mu\text{m}$ nozzle with a backing pressure of 20 bar and collimated in a two stage jet. A density

of 5×10^{11} atoms/cm² and a diameter of 1.5 mm were achieved. The active cooling by the supersonic expansion in expansion direction combined with passive one in the perpendicular direction by the geometry resulted in a 3 dimensional cold target and a momentum uncertainty below 0.1 a.u.

At the intersection volume where proton and helium beam were intersected, electrons and ions were created. A weak electrostatic field of 4.8 V/cm was applied to project electrons and recoiling ions onto two position and time sensitive detectors. To optimize the resolution, a three dimensional time and space focusing geometry [18, 19] was used for the recoil ion arm of the spectrometer. The ion were detected by a 80 mm diameter micro channel plate (MCP) detector with delay-line anode [20, 21]. The time focusing was realized using a field free drift tube [22], while an adjustable electrostatic lens was used to achieve space focusing. This lens was optimized by minimizing the spatial width of the lines on the detector from He⁺ ions created by pure capture, which have been recorded parallel to the transfer ionization events (for an example see Fig. 1 in [23] or Fig. 1 in [12]). A momentum resolution of 0.1 a. u. was achieved in all three directions. The electrons were guided by a magnetic field (see [24]) of 15 and 25 Gauss and accelerated over a length of 20 cm by the same electric field in a time focusing geometry (40 cm additional field free drift tube) onto a MCP detector of 120 mm active diameter. The overall spectrometer geometry, especially the ion's part was simulated using SIMION to gain the maximum resolution and efficiency.

We reached an overall acceptance of 4π solid angle for recoil ions up to a momentum of 10 a.u. and electrons up to 6 a.u. A three-particle coincidence ($H^0 + He^{2+} + e$) was applied to record the data event by event. From the positions of impact on the detectors and the time-of-flight we can derive the initial momentum vectors of the recoil ion and the electron. The projectile transverse momentum vectors were directly measured. Checking energy and momentum conservation the background was strongly suppressed during the off-line data analysis. Also the overall resolution was good enough to measure the final electronic state of the H and separate events where the hydrogen was found in the ground state from where the electron was captured into an excited state. Only these events, where the hydrogen is in the ground state are presented in the following.

III. THEORY

As stated above, we consider the He atom as a target for the TI reaction. We follow definitions and notations given in [10] and not repeat all conditions here. In the momentum representation in the lab frame and at very small scattering angle θ_p the symmetrized matrix element is given by

$$\begin{aligned} \mathcal{T}_{FBA} = -4\pi\sqrt{2} \int \frac{d\vec{x}}{(2\pi)^3} \frac{\tilde{\phi}_H(x)}{|\vec{v}_p - \vec{q} - \vec{x}|^2} [F(\vec{q}; 0; \vec{k}) + F(\vec{v}_p - \vec{x}; -\vec{v}_p + \vec{q} + \vec{x}; \vec{k}) \\ - 2F(\vec{v}_p - \vec{x}; 0; \vec{k})] = A1 + A2 + A3, \end{aligned} \quad (1)$$

where

$$F(\vec{y}; \vec{\eta}; \vec{k}) = \int e^{-i\vec{y}\vec{r}_1 - i\vec{\eta}\vec{r}_2} \varphi_c^{-*}(\vec{k}, \vec{r}_2) \Phi_0(\vec{r}_1, \vec{r}_2) d\vec{r}_1 d\vec{r}_2, \quad (2)$$

\vec{v}_p is the fast proton velocity, the transferred momentum $\vec{q} = \vec{p}_H - \vec{p}_p$, \vec{k} the electron momentum, $\Phi_0(\vec{r}_1, \vec{r}_2)$ the helium ground wave function, and the Coulomb wave function of the final target ion

$$\varphi_c^{-*}(\vec{k}, \vec{r}) = e^{-\pi\xi/2} \Gamma(1 + i\xi) e^{-i\vec{k}\vec{r}} {}_1F_1(-i\xi, 1; ikr + i\vec{k}\vec{r}); \quad \xi = -2/k.$$

The FDSC is calculated by the formula

$$\frac{d^2\sigma}{dk_\perp dk_\parallel} = \frac{m^2 k_\perp}{(2\pi)^4} \int_0^{\theta_{max}} \theta_p d\theta_p \int_0^{2\pi} d\phi_k |A1 + A2 + A3|^2, \quad (3)$$

with $m = 1836.15$ being the proton mass. We display all vectors' components for clarity: $\vec{v}_p = \{0, 0, v_p\}$, $\vec{q} = \{mv_p\theta_p, 0, q_\parallel\}$, $\vec{k} = \{k_\perp \cos \phi_k, k_\perp \sin \phi_k, k_\parallel\}$. We also remind that $q_\parallel = v_p/2 + Q/v_p$ with $Q = E_0^{He} - E^H - k^2/2$.

In (1) the term A_1 is the OBK amplitude, where any trial helium wave function can be used. The amplitude A_3 can also be attributed to SO. It describes the contribution of heavy particles interaction and was discussed in the Introduction. The amplitude A_2 is a typical PWFBA realization of the BE mechanism.

IV. RESULTS AND DISCUSSION

For calculations we use three trial helium wave functions. One is the loosely correlated $1s^2$ Roothaan-Haartree-Fock (RHF) function of Clementi and Roetti [25] ($E_0^{He} = -2.8617$).

The two others are a highly correlated function of the type

$$\Psi(r_1, r_2, r_{12}) = \sum_{j=1}^N D_j [\exp(-\alpha_j r_1 - \beta_j r_2) + \exp(-\alpha_j r_2 - \beta_j r_1)] \exp(-\gamma_j r_{12}), \quad (4)$$

which was described in [26] ($E_0^{He} = -2.9037$), and the configuration interaction (CI) wave function of Mitroy [27] ($E_0^{He} = -2.9031$).

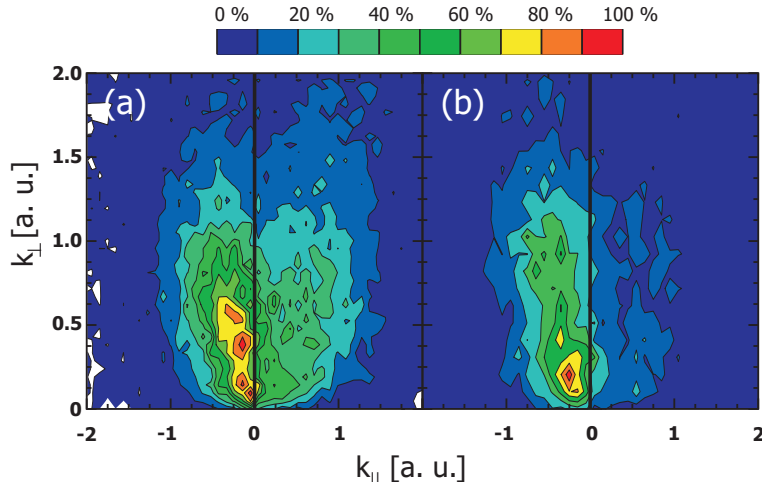


FIG. 1: (Color online) Experimental momentum distribution of the electron for a) $E_p = 300$ keV and b) $E_p = 630$ keV. The projectile is moving in the positive $k_{||}$ direction, i. e. from the left to the right. The data are integrated over all other observables, i. e. the integral over the shown distribution corresponds to the total transfer ionization cross section for the H(n=1) state.

The experimental data at $E_p = 300$ and $E_p = 630$ keV, shown in Figure 1, display a noticeable peak at backward (negative $k_{||}$) direction and a less resolved peak at forward direction (positive $k_{||}$). The forward peak structure has more intensity at the lower projectile energy of 300 keV, as the projectile-target interaction time is longer and therefore an additional interaction, the electron knock-off, more likely to occur.

As expected calculations with the loosely correlated wave function [Figs. 2(c) and 2(d)] give practically no backward peak to the electron's distribution. Both highly correlated helium wave functions give very similar distributions [Figs. 2(a) and 2(b)], which include both forward and backward peaks. However, visually they are hard to compare with the experiment.

To avoid effects of color scales, we present additionally two slices of these distributions at $E_p = 300$ keV and fixed k_{\perp} : $k_{\perp} = 0.2$ in Fig. 3(a) and $k_{\perp} = 0.4$ in Fig. 3(b). The experimental

points are normalized to the theory's peak maximum along the whole distributions. First, we clearly see that both used correlated wave functions give practically the same curves. Second, theory and experiment well coincide at negative k_{\parallel} , what clearly demonstrate that the PWFBA shake-off amplitude is quite sufficient to describe the backward peak. This requires of course, the use of highly correlated target wave functions. Third, we see that the theory noticeably exceeds the experimental points in the forward domain $k_{\parallel} > 0$. It is a clear indication that the SBA calculations are needed here. Unfortunately, we cannot provide these calculations at the moment.

We finally show a comparison of the total transfer ionization cross section in PWFBA theory, using Mitroy helium wave function, and experiment. In Figure 4 the agreement is quite satisfactory over a wide range of the proton energies.

V. CONCLUSIONS

In conclusion, we presented highly differential theory (PWFBA) and experimental data from a kinematical complete experiment on transfer ionization in proton-Helium-collision at 300 and 630 keV. The observed splitting into forward and backward emission originates from two different contributions, the A_2 -term (binary encounter) and the $A_1 + A_3$ -term (shake-off). Comparison of loosely and highly correlated wave functions for the initial state confirms the high sensitivity of the experiment to the subtle features of the initial state wave function. Better agreement for the forward emitted electrons can be expected for calculations in the second order. At the same time, backward emitted electrons can be described within the first Born approximation at high projectile energies.

VI. ACKNOWLEDGEMENTS

We acknowledge financial support from the Deutsche Forschungsgemeinschaft (DFG), Grant No. SCHO 1210/2-1. As well this work partially supported by Russian Foundation of Basic Research (RFBR), Grant No. 11-01-00523-a. All calculations were performed using Moscow State University Research Computing Centre (supercomputers Lomonosov and Chebyshev) and Joint Institute for Nuclear Research Central Information and Computer

Complex. The authors are grateful to K. Kouzakov for inspiring discussions and help.

- [1] J. S. Briggs and V. Schmidt, *J. Phys. B: At. Mol. Opt. Phys.*, **33**, R1, (2000)
- [2] A. Knapp, A. Kheifets, I. Bray, Th. Weber, A. L. Landers, S. Schössler, T. Jahnke, J. Nickles, S. Kammer, O. Jagutzki, L. Ph. Schmidt, T. Osipov, J. Rösch, M. H. Prior, H. Schmidt-Böcking, C. L. Cocke and R. Dörner, *Phys. Rev. Lett.*, **89**, 033004, (2002)
- [3] J. R. Oppenheimer, *Phys. Rev.*, **31**, 349 (1928); H. C. Brinkman and H. A. Kramers, *Proc. Acad. Sci. Amsterdam*, **33**, 973 (1930).
- [4] L. H. Thomas, *Proc. Roy. Soc. A*, **114**, 561 (1927)
- [5] E. Weigold and I. E. McCarthy, *Electron Momentum Spectroscopy* (Kluwer Academic/Plenum, New York, 1999); V. G. Neudatchin, Yu. V. Popov, and Yu. F. Smirnov, *Phys. Usp.*, **42**, 1017 (1999).
- [6] Yu.V. Popov, O. Chuluunbaatar, S.I. Vinitsky, L.U. Ancarani, C. Dal Cappello, and P.S. Vinitsky, *JETP*, **95**, 620 (2002).
- [7] N. Watanabe, Y. Khajuria, M. Takahashi, Y. Udagawa, P. S. Vinitsky, Yu. V. Popov, O. Chuluunbaatar, and K. A. Kouzakov, *Phys. Rev. A* **72**, 032705 (2005).
- [8] A. B. Voitkiv, B. Najjari and J. Ullrich, *Phys. Rev. Lett.*, **101**, 223201, (2008)
- [9] M. Schulz, X. Wang, M. Gundmundsson, K. Schneider, A. Kelkar, A. B. Voitkiv, B. Najjari, M. Schöffler, L. Ph. H. Schmidt, R. Dörner, J. Ullrich, R. Moshhammer and D. Fischer, *Phys. Rev. Lett.*, **108**, 043202, (2012)
- [10] S. Houamer, Yu.V. Popov, and C. Dal Cappello, *Phys. Rev. A* **81**, 032703 (2010).
- [11] J.S. Briggs and K. Taulbjerg, *J. Phys. B: At. Mol. Phys.*, **12**, 2565, (1979)
- [12] Hong-Keun Kim, M.S. Schoeffler, S. Houamer, O. Chuluunbaatar, J.N. Titze, L.Ph.H. Schmidt, T. Jahnke, H. Schmidt-Boecking, A. Galstyan, Yu. V. Popov, and R. Doerner, *Phys. Rev. A*. **85**, 022707 (2012)
- [13] Dž. Belkić, R. Gayet, and A. Salin, *Phys. Rep.* **56**, 279 (1979).
- [14] M. S. Schöffler, O. Chuluunbaatar, Yu. V. Popov, S. Houamer, J. Titze, T. Jahnke, L. Ph. H. Schmidt, O. Jagutzki, A. G. Galstyan and A. A. Gusev, *Phys. Rev. A.*, **87**, 032715, (2013)
- [15] J. Ullrich, R. Moshhammer, R. Dörner, O. Jagutzki, V. Mergel, H. Schmidt-Böcking and L. Spielberger, *J. Phys. B: At. Mol. Opt. Phys.*, **30**, 2917, (1997)

- [16] R. Dörner, V. Mergel, O. Jagutzki, L. Spielberger, J. Ullrich, R. Moshhammer and H. Schmidt-Böcking, *Physics Reports*, **330**, 95, (2000)
- [17] J. Ullrich, R. Moshhammer, A. Dorn, R. Dörner, L. Ph. H.Schmidt and H. Schmidt-Böcking, *Rep. Prog. Phys.*, **66**, 1463, (2003)
- [18] M. S. Schöffler, T. Jahnke, J. Titze, N. Petridis, K. Cole, L. Ph. H. Schmidt, A. Czasch, O. Jagutzki, J. B. Williams, C. C. Cocke, T. Osipov, S. Lee, M. H. Prior, A. Belkacem, A. L. Landers, H. Schmidt-Böcking, R. Dörner, and Th. Weber, *New Journal of Physics*, **13**, 095013, (2011)
- [19] V. Mergel, R. Dörner, J. Ullrich, O. Jagutzki, S. Lencinas, S. Nüttgens, L. Spielberger, M. Unverzagt, C. L. Cocke, R. E. Olson, M. Schulz, U. Buck, E. Zanger, W. Theisinger, M. Isser, S. Geis, H. Schmidt-Böcking, *Phys. Rev. Lett.*, **74**, 2200, (1995)
- [20] O. Jagutzki, J. S. Lapington, L. B. C. Worth, U. Spillman, V. Mergel and H. Schmidt-Böcking, *Nucl. Instr. and Meth. in Phys. Res. A*, **477**, 256, (2002)
- [21] O. Jagutzki, V. Mergel, K. Ullmann-Pfleger, L. Spielberger, U. Spillmann, R. Dörner and H. Schmidt-Böcking, *Nucl. Instr. and Meth. in Phys. Res. A*, **477**, 244, (2002)
- [22] W. C. Wiley, I. H. McLaren, *Rev. Sci. Instr.*, **26**, 1150, (1955)
- [23] M. S. Schöffler, J. Titze, L. Ph. H. Schmidt, T. Jahnke, N. Neumann, O. Jagutzki, H. Schmidt-Böcking, R. Dörner, and I. Mancev, *Phys. Rev. A*, **79**, 064701, (2009)
- [24] R. Moshhammer, M. Unverzagt, W. Schmitt, J. Ullrich, and H. Schmidt-Böcking, *Nucl. Instr. Meth.*, **B 108**, 425, (1996)
- [25] Enrico Clementi and Carla Roetti, *Atomic Data and Nuclear Data Tables* **14**, 177 (1974).
- [26] O. Chuluunbaatar, I.V. Puzinin, P.S. Vinitzky, Yu.V. Popov, K.A. Kouzakov, and C. Dal Cappello, *Phys. Rev. A* **74**, 014703 (2006).
- [27] J. Mitroy, I.E. McCarthy, and E. Weigold, *J. Phys. B: At. Mol. Opt. Phys.* **18**, 4149 (1985)
- [28] M.B. Shah and H.B. Gilbody, *J. Phys. B: At. Mol. Phys.* **18**, 899 (1985).
- [29] V. Mergel, R. Dörner, M. Achler, Kh. Khayyat, S. Lencinas, J. Euler, O. Jagutzki, S. Nüttgens, M. Unverzagt, L. Spielberger, W. Wu, R. Ali, J. Ullrich, H. Cederquist, A. Salin, C.J. Wood, R.E. Olson, Dž. Belkić, C.L. Cocke, and H. Schmidt-Böcking, *Phys. Rev. Lett.* **79**, 387 (1997).
- [30] H.T. Schmidt, J. Jensen, P. Reinhed, R. Schuch, K. Støchkel, H. Zettergren, H. Cederquist, L. Bagge, H. Danared, A. Källberg, H. Schmidt-Böcking, and C.L. Cocke, *Phys. Rev. A* **72**, 012713 (2005).

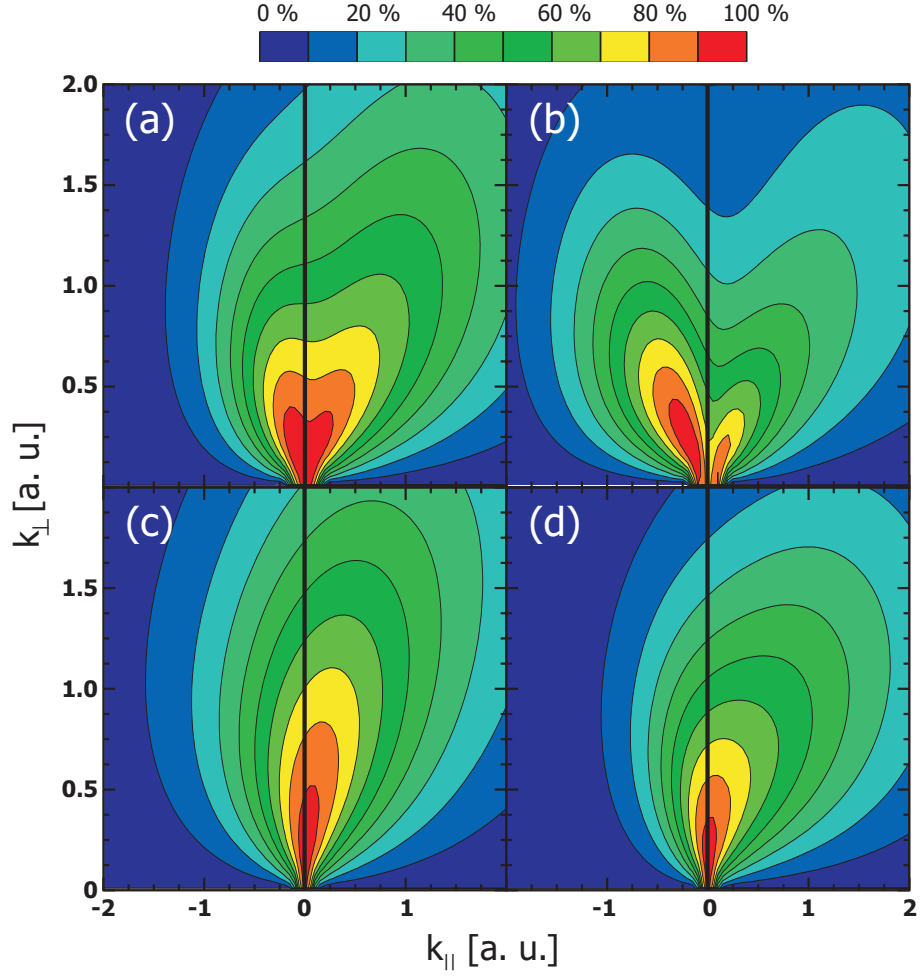


FIG. 2: Calculated electron momentum distribution longitudinal vs. transversal within the PWFBA for a) $E_p = 300$ keV with strong correlation, b) $E_p = 630$ keV with strong correlation, c) $E_p = 300$ keV with weak correlation, d) $E_p = 630$ keV with weak correlation

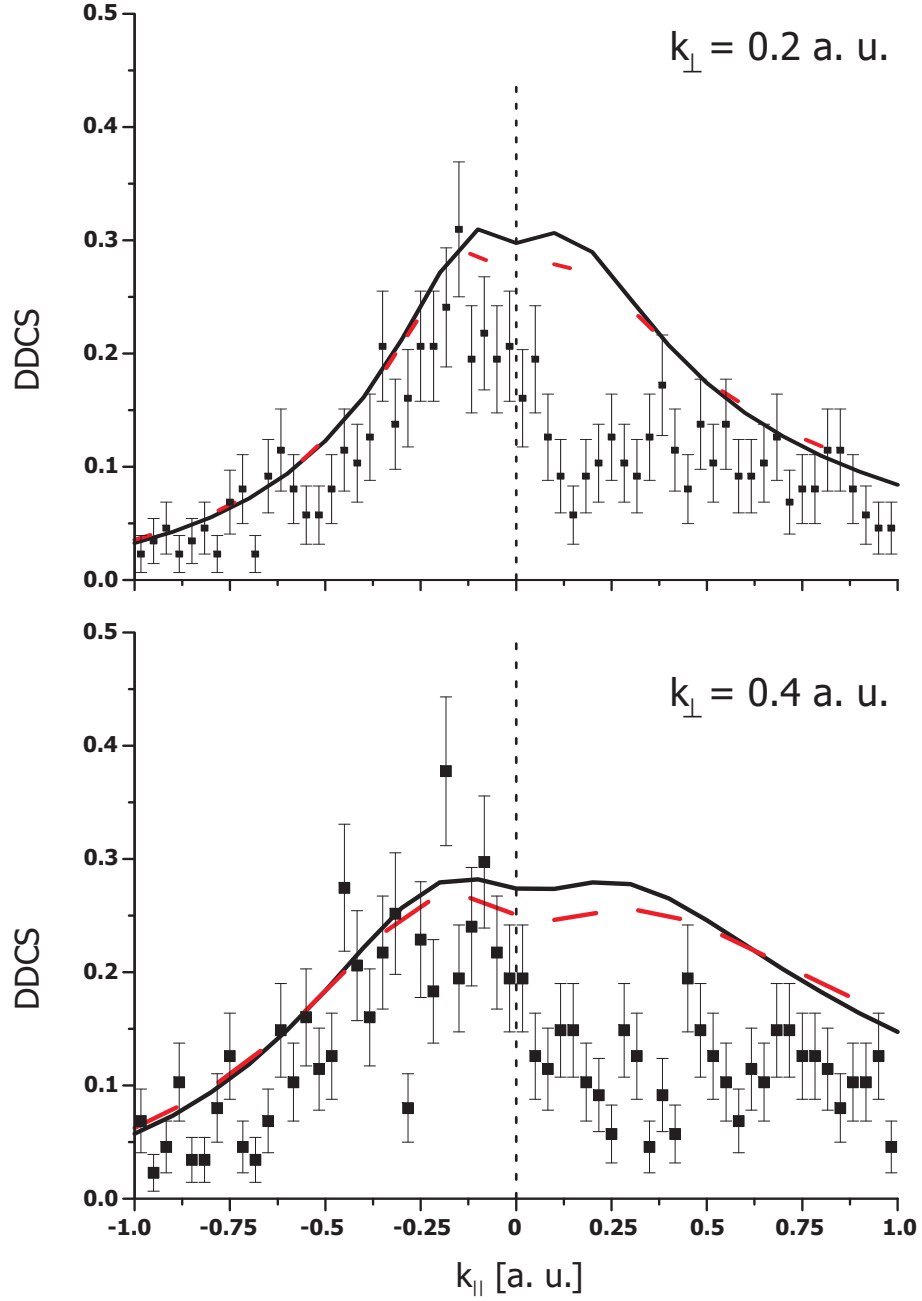


FIG. 3: DDSCS versus $k_{||}$ at $E_p = 300$ keV for fixed $k_{\perp} = 0.2$ (top), $k_{\perp} = 0.4$ (bottom). Solid line, highly correlated wave function [26]; dashed line, that of Mitroy. Dots are experimental points.

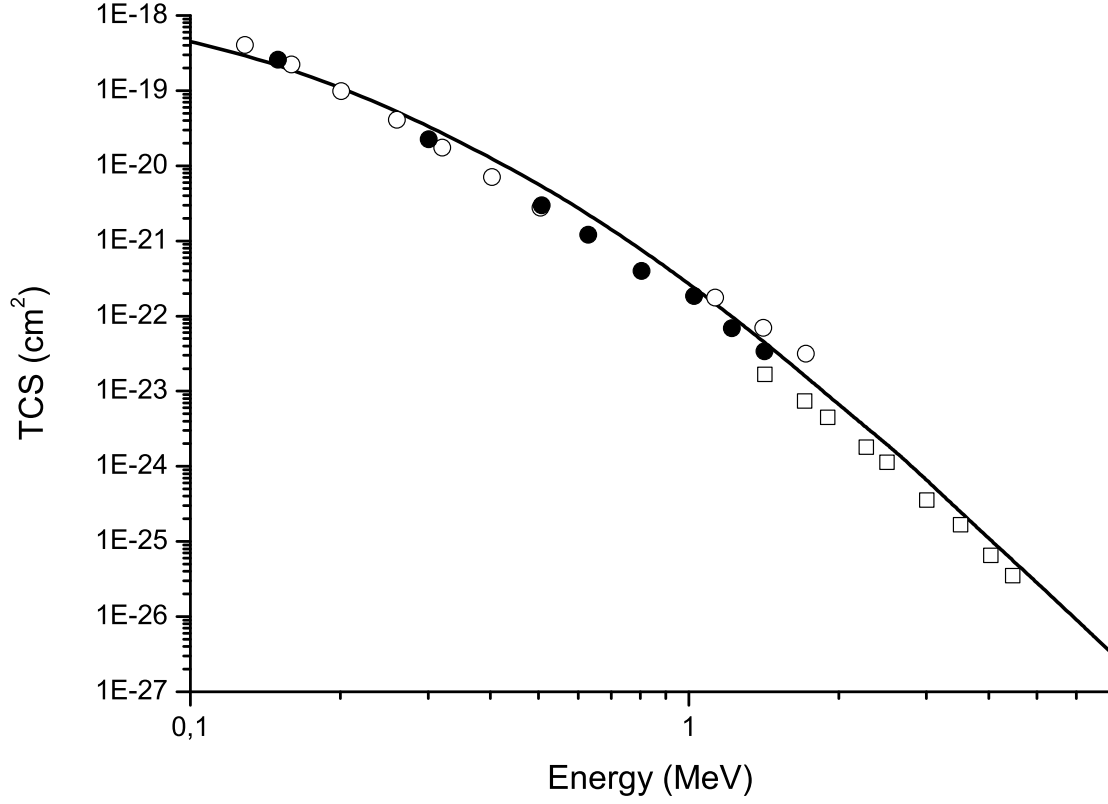


FIG. 4: Total cross section for transfer ionization for different proton energies E_p (solid line), using Mitroy wave function. Experiment: open circles, Shah and Gilbody [28]; full circles, Mergel et al. [29]; open squares, Schmidt et al [30]